

Jointly Optimised Iterative Source-coding, Channel-coding and Modulation for Transmission over Wireless Channels

S. X. Ng, F. Guo, J. Wang, L-L. Yang and L. Hanzo

School of ECS, University of Southampton, SO17 1BJ, UK.

Tel: +44-23-8059 3125, Fax: +44-23-8059 4508

Email: {sxn,fg01r,jw02r,lly,lh}@ecs.soton.ac.uk, <http://www-mobile.ecs.soton.ac.uk>

Abstract – Joint source-coding, channel-coding and modulation schemes based on Variable Length Codes (VLCs), Trellis Coded Modulation (TCM), Turbo TCM (TTCM), Bit-Interleaved Coded Modulation (BICM) and iteratively decoded BICM (BICM-ID) schemes are proposed. A significant coding gain is achieved without bandwidth expansion, when exchanging information between the VLC and the coded modulation decoders with the advent of iterative decoding. With the aid of using independent interleavers for the In-phase and Quadrature phase components of the complex-valued constellation, further diversity gain may be achieved. The performance of the proposed schemes is evaluated when communicating over both AWGN and Rayleigh fading channels. Explicitly, at BER= 10^{-5} most of the proposed schemes have BER curves around 2 dBs away from the channel capacity limit.

1. INTRODUCTION

Trellis Coded Modulation (TCM) [1, 2] and Turbo TCM (TTCM) [2, 3] constitute bandwidth-efficient joint channel coding and modulation schemes, which were originally designed for transmission over Additive White Gaussian Noise (AWGN) channels. Set Partitioning (SP) based phasor constellation labelling was used in these schemes in order to increase the minimum Euclidean distance between the encoded information bits in the signal-space. A symbol-based turbo interleaver and a symbol-based channel interleaver were utilised for the sake of achieving time diversity, when communicating over Rayleigh fading channels. Another powerful Coded Modulation (CM) scheme utilising bit-based channel interleaving in conjunction with Gray signal labelling, which is referred to as Bit-Interleaved Coded Modulation (BICM), was proposed in [4, 5]. It combines conventional non-systematic convolutional codes with several independent bit interleavers. The number of parallel bit-interleavers used equals the number of channel coded bits in a symbol [2, 4]. Recently, iteratively decoded BICM using SP based signal labelling, referred to as BICM-ID has also been proposed [6].

In an effort to increase the achievable time diversity, a multidimensional TCM scheme utilising a symbol interleaver and two encoders was proposed in [7], where the individual encoders generate the In-phase (I) and Quadrature-phase (Q) components of the complex transmitted signal, respectively. Another TCM scheme using constellation rotation was proposed in [8], which utilised two separate channel interleavers for interleaving the I and Q components of the complex transmitted signals, but assumed the absence of I/Q *cross-coupling*, when communicating over Rayleigh fading channels. Explicitly, I/Q cross-coupling is the phenomenon imposed by convolv-

ing the transmitted signal with the complex-valued Channel Impulse Response (CIR) where the I (or Q) component of the received signal becomes dependent on both the I and Q components of the transmitted signals. The technique of invoking separate I and Q interleaving and optimally rotating the constellation in order to increase the achievable diversity gain was first proposed in [9]. This type of diversity was referred to as modulation diversity or signal-space diversity in [10], where a significant performance improvement was achieved in the context of both an uncoded system [10] as well as in a TCM scheme [8]. Recently, a new approach which amalgamates Space-Time Block Coding (STBC) [11] with IQ-interleaved CM (STBC-IQ-CM) schemes using no constellation rotation was proposed, which is suitable for transmission over both AWGN as well as Rayleigh fading channels imposing I/Q cross-coupling [12, 13]. The diversity achieved with the advent of IQ-interleaving without constellation rotation was referred to as IQ-diversity in [12, 13]. It was shown in [12] that the STBC-IQ-based TCM/TTCM scheme is capable of quadrupling the achievable diversity potential of conventional single-transmitter based symbol-interleaved TCM/TTCM, when communicating over narrowband uncorrelated Rayleigh fading channels *without compromising the coding gain attainable over AWGN channels*. Furthermore, the STBC-IQ-BICM-ID scheme of [13] is also capable of benefiting from IQ-interleaving owing to employing iterative detection and SP-based phasor constellation labelling.

Lossless Variable Length Codes (VLCs) constitute a family of low-complexity source compression schemes. In order to exploit the residual redundancy of VLCs, numerous trellis-based VLC decoding techniques have been proposed, such as the joint source/channel coding scheme of [14], where the VLC decoder uses the bit-based trellis structure of [15]. Explicitly, in [14] a reversible VLC [16] was invoked as the outer code and a convolutional code was utilised as the inner code. However, the explicit knowledge of the number of VLC output bits per transmission frame is required for the VLC's bit-based trellis decoding, which has to be signalled to the decoder, reducing both the compression efficiency and the error resilience.

In order to improve the bandwidth and power efficiency of the joint source/channel coding scheme contrived in [14], *in this contribution we proposed the novel concept of amalgamated source-coding, channel-coding and modulation*. The performance benefits of the scheme will be demonstrated in the context of a range of CM arrangements, namely TCM-VLC, TTCM-VLC, BICM-VLC and BICM-ID-VLC, which invokes TCM, TTCM, BICM and BICM-ID coded modulation as the inner constituent code. Note that unlike the iterative BICM-ID scheme, the non-iterative BICM scheme of [13] does not benefit from IQ-interleaving. Therefore, in our investigations we will also invoke the IQ-TCM, IQ-TTCM and IQ-BICM-ID scheme of [13] as the inner constituent code for the sake of attaining additional IQ-diversity, when communicating over Rayleigh fading channels. Note that the signal-space diversity or IQ-diversity has also been incorpo-

The financial support of both the EPSRC, Swindon UK and the EU under the auspices of the Phoenix project is gratefully acknowledged.

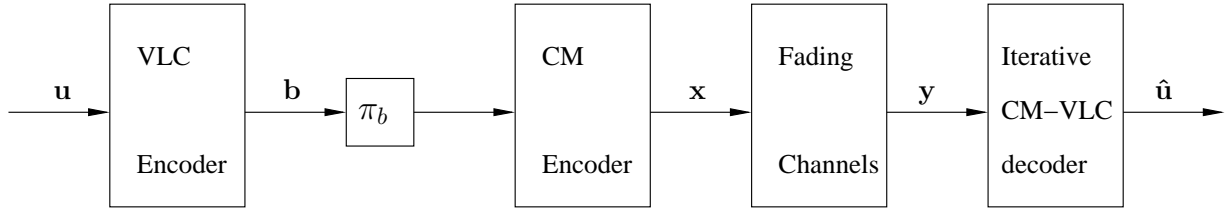


Figure 1: Block diagram of the CM-VLC scheme. The notations \mathbf{u} , $\hat{\mathbf{u}}$, \mathbf{b} , \mathbf{x} , \mathbf{y} and π_b denote the vectors of the source symbols, the estimates of the source symbols, the VLC coded bits, the CM coded symbols, the received symbols and the bit interleaver, respectively.

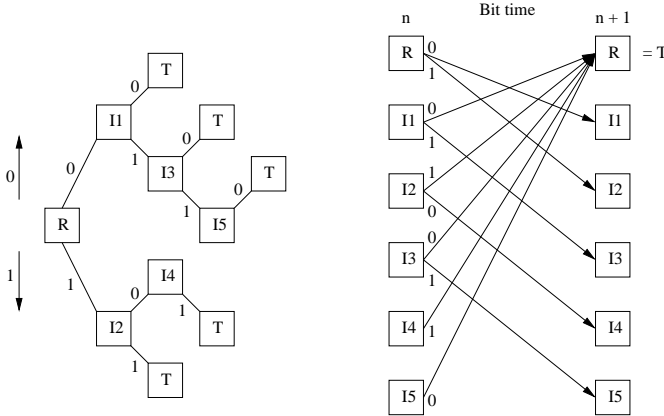


Figure 2: Code-tree and trellis for the VLC $C = \{00, 11, 010, 101, 0110\}$ [15] ©IEEE, 1997, Balakirsky.

rated into the BICM-ID scheme of [17] where an un-rotated 16-level Quadrature Amplitude Modulation (16QAM) constellation and a half-rate non-systematic convolutional code were employed for communicating over uncorrelated Rayleigh fading channels imposing no I/Q cross-coupling.

2. SYSTEM OVERVIEW

We employ the reversible VLC codes from [16], where the codewords are $C = \{00, 11, 010, 101, 0110\}$ associated with the source symbol sequence of $u = \{0, 1, 2, 3, 4\}$. Specifically, the longest VLC codeword length is $l_{max} = 4$. The associated entropy is 2.14 bits/symbol and the average codeword length is 2.46 bits, giving a coding rate of $R_{vlc} = 2.14/2.46 = 0.87$. The VLC outer encoder of Figure 1 maps the source symbol u to a variable-length codeword, which can be represented as a binary bit sequence $\mathbf{b} = \{b_1, b_2, \dots, b_l\}$ of length l , where $l \leq l_{max}$, at each encoding instance. However, we fix the VLC encoder's total bit sequence length to L_{bit} , in the range of $(2048m - l_{max}) \leq (L_{bit} + L_{side}) \leq 2048m$, where m is the number of original VLC-encoded bits per CM coded symbol, l_{max} is the longest VLC codeword length and L_{side} is the number of bits required for conveying the side information related to the number of VLC output bits per transmission frame to the VLC decoder. Furthermore, L_{dummy} number of zero-valued dummy bits are concatenated to the VLC output bit sequence, such that we have $L_{bit} + L_{dummy} + L_{side} = 2048m$ bits. In an effort to render our investigations as realistic as possible, the side information related to the number of VLC output bits per transmission frame conveying the VLCs is explicitly signalled to the decoder by repeating the bits three times for the sake of majority logic based detection and then further protected by the CM scheme. The resultant $2048m$ number of bits

representing the VLC output bits, dummy bits and side information bits are treated as input bits of the CM encoder, which has a coding rate of $R_{cm} = \frac{m}{m+1}$ and employs a 2^{m+1} -level modulation scheme.

The tree structure of the VLC $C = \{00, 11, 010, 101, 0110\}$ used in our investigations is shown at the left of Figure 2, where the nodes in the tree are subdivided into a so-called root-node (R), internal nodes (I) and terminal nodes (T) according to [15]. A section of the corresponding trellis diagram between the bit time instants n and $n+1$ is illustrated at the right of Figure 2. Explicitly, there is a single root state which corresponds to the root node R of the code tree and a number of further states, that are labelled by the internal nodes I1...I5 of the tree. All terminal nodes lead again to the root state R=T of Figure 2. This is a relatively simple and time-invariant trellis structure. For a VLC sequence, which consists of N bits, the trellis can be terminated after N sections. Since the trellis describing the VLC source code can be considered as the trellis of a channel code, which consists of code words having a length of N , the bit-based Maximum A Posteriori Probability (MAP) [2] algorithm can be used for computing the *a posteriori* probability for each bit value and then fed back to the coded modulation decoder.

The novel decoder structure of the (IQ-)TTCM-VLC scheme is illustrated in Figure 3, where there are three constituent decoders, each labelled with a round-bracketed index. Symbol-based and bit-based MAP algorithms [2] operating in the logarithmic-domain are employed by the TCM decoders and by the VLC decoder, respectively. The notations P , S , A and E denote the logarithmic-domain probabilities of the parity information, the systematic information, the *a priori* information and the *extrinsic* information, respectively. The notations L_p , L_e and L_i denote the Logarithmic-Likelihood Ratio (LLR) of the *a posteriori*, *extrinsic* and *intrinsic* information, respectively. The probabilities or LLRs associated with one of the three constituent decoders having a label of 1...3 are differentiated by the superscript of 1...3. The logarithmic-domain symbol probabilities of the IQ-interleaved or symbol-interleaved TTCM-coded symbols are computed by the demodulator based on the approach of [12]. There are 2^{m+1} probabilities associated with an $(m+1)$ -bit TTCM-coded symbol, which have to be determined for the MAP decoder [2]. These probabilities are input to the TTCM MAP decoder as $[P\&S]$, which indicates the inseparable nature of the parity and systematic information [2, 3]. The *a posteriori* information of the m -bit systematic part of an $(m+1)$ -bit TTCM symbol at the output of a constituent TCM decoder can be separated into two components (Section 9.4 [2] and [3]): 1) the inseparable *extrinsic* and systematic component $[E\&S]$ also referred to as the *intrinsic* component, which is generated by one of the constituent TCM decoders, and 2) the *a priori* component A , which is provided by the other constituent TCM decoder. However, in our proposed scheme the *a priori* component A comprises also the additional *extrinsic* information provided by the constituent VLC decoder, namely E^3 , as we can see from Figure 3. Explicitly, we have $A^{(1,2)} = [E\&S]^{(2,1)} + E^3$,

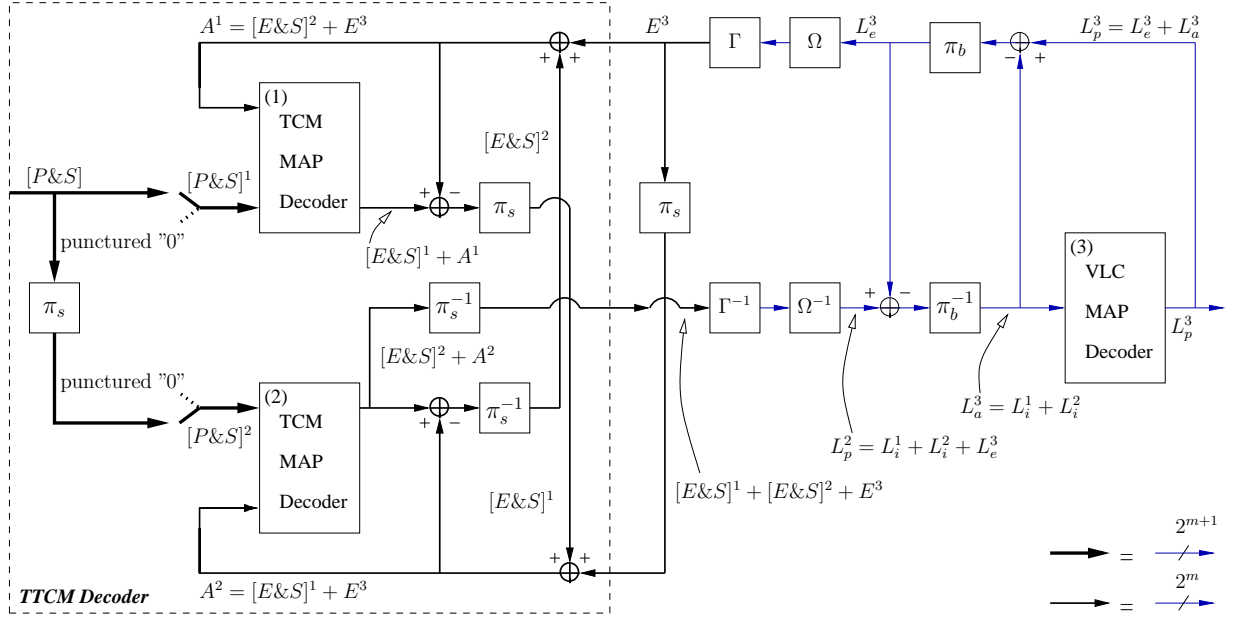


Figure 3: Block diagram of the (IQ-)TTCM-VLC scheme. The notations $\pi_{(s,b)}$ and $\pi_{(s,b)}^{-1}$ denote the interleaver and deinterleaver, while the subscript s or b denote the symbol-based or bit-based nature of the interleaver, respectively. Furthermore, Γ and Γ^{-1} denote LLR-to-symbol and symbol-to-LLR probability conversion, while Ω and Ω^{-1} denote the addition and deletion of the LLRs of the side information and dummy bits.

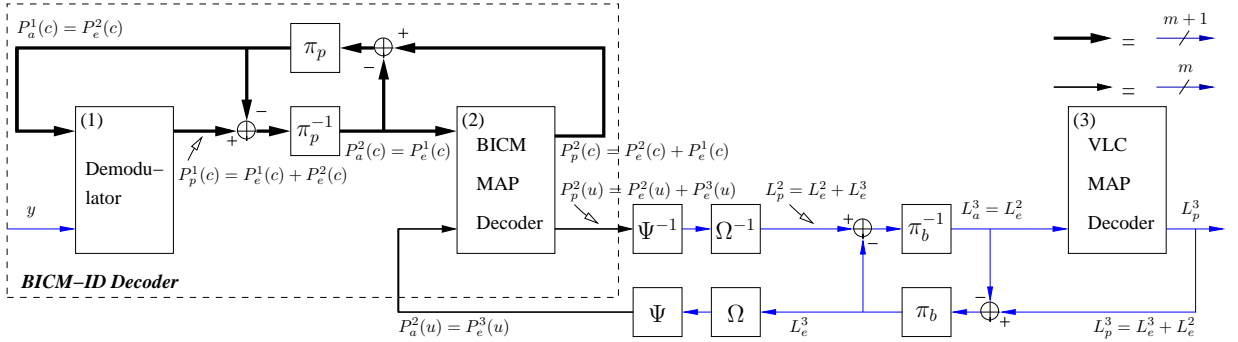


Figure 4: Block diagram of the (IQ-)BICM-ID-VLC scheme. The notations π_p and π_b denote the BICM scheme's independent parallel bit interleavers and the VLC scheme's bit interleaver, respectively, while π^{-1} denotes bit deinterleaver. Furthermore, Ψ and Ψ^{-1} denote serial-to-parallel and parallel-to-serial conversion, while Ω and Ω^{-1} denote the addition and deletion of the LLRs of the side information and dummy bits.

where the extrinsic component E^3 contributing to A^2 is the symbol-interleaved version of E^3 contributing to A^1 . The *a posteriori* information of the m -bit systematic part of an $(m+1)$ -bit TTCM symbol provided by the second TCM decoder is then symbol-deinterleaved and converted to LLRs.

At the commencement of VLC decoding, the side information conveying the number of VLC output bits in the transmission frame has to be extracted. Hence, based on the side information segment of the TTCM decoded *a posteriori* LLRs, the number of dummy bits and the number of VLC output bits has to be calculated. Then only the *a posteriori* LLRs associated with the VLC bit sequence are passed on to the VLC decoder. The *a priori* LLR of a VLC-coded bit is constituted by the sum of the *intrinsic* LLRs of both TCM decoders, which is shown in Figure 3 as $L_a^3 = L_i^1 + L_i^2$. Based on L_a^3 and on the calculated number of VLC output bits, the bit-based VLC MAP decoder computes the *a posteriori* LLR as $L_p^3 = L_e^3 + L_i^1 + L_i^2$.

Only the *extrinsic* LLR L_e^3 is passed back to the TTCM decoder. The VLC decoder's extrinsic LLR L_e^3 is concatenated with the LLRs of the side information, where the latter component is represented by zeros in the LLR-domain, since the corresponding probabilities are assumed to be 0.5. Furthermore, the LLRs of the dummy zero bits are concatenated as large negative LLR values. Finally, LLR-to-symbol probability conversion is invoked for generating E^3 . At the final outer iteration, a maximum likelihood sequence estimation based on L_p^3 is invoked for yielding the original uncoded information bits. By the same token, an (IQ-)TTCM-VLC decoder structure is similar to that of Figure 3, with the simplification that the second TCM decoder is removed and the *a posteriori* information of the first TCM decoder is passed directly to the symbol-to-LLR probability converter.

Let us now consider the novel decoder structure of the (IQ-) BICM-ID-VLC scheme of Figure 4, which consists of three components and each is labelled with a round-bracketed index. Bit-based MAP algo-

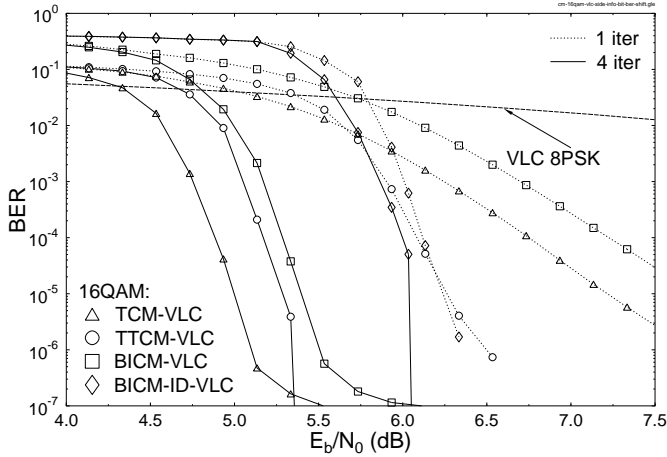


Figure 5: BER versus E_b/N_0 performance of the proposed 16QAM-based CM-VLC schemes and VLC 8PSK, when communicating over **AWGN channels**. All of these schemes have an effective throughput of **2.61 BPS**.

gorithms [2] operating in the logarithmic-domain are employed by the BICM decoders and by the VLC decoder. The notations $P(c)$ and $P(u)$ denote the LLRs of the $m + 1$ coded bits and the m uncoded information bits of the BICM scheme, respectively. The subscripts of p , e , a and i denote the *a posteriori*, *extrinsic*, *a priori* and *intrinsic* nature of the LLR, respectively. Again, the superscripts of $1 \dots 3$ represent the associated constituent components having a label of $1 \dots 3$. Note that if a systematic convolutional code is employed by the BICM encoder, we have $P_p^2(u) = P_i^2(u) + P_e^3(u)$, where $P_i^2(u)$ denotes the *intrinsic* LLRs of the uncoded information bits representing the *extrinsic* information provided by the decoder itself and the systematic information obtained from the systematic part of $P_e^1(c)$. By contrast, for a BICM scheme employing a non-systematic convolutional code, we have $P_p^2(u) = P_e^2(u) + P_e^3(u)$, since no systematic information accrues from $P_e^1(c)$. However, the computation of $P_e^2(u)$ is still dependent on $P_e^1(c)$. Similarly, the computation of $P_e^3(c)$ is also dependent on $P_e^1(u)$. The LLR probabilities of the IQ-BICM-ID and BICM-ID are computed by the demodulator based on the approach of [12]. On the other hand, the BICM-VLC decoder structure is similar to that of Figure 4, with the simplification that there is no internal iteration between the demodulator and the BICM decoder.

3. SIMULATION RESULTS

We evaluated the performance of the proposed schemes using both 4-level Quadrature Amplitude Modulation (4QAM) and 16-level QAM (16QAM) in the context of the 64-state TCM scheme of [1], the 64-state BICM scheme of [4] as well as invoking an iterative 8-state TCM arrangement using four decoding iterations [3] and an 8-state BICM-ID arrangement employing eight decoding iterations [6]. These CM parameters were chosen for the sake of maintaining a similar decoding complexity, since the total number of trellis-stages was identical [12]. We also set the maximum number of outer iterations between the CM decoder and the VLC decoder to four, where an outer iteration is constituted by one CM decoding and one VLC decoding operation. The effective throughput of the system is $1 \times R_{vlc} = 0.87$ and $3 \times R_{vlc} = 2.61$ Bit Per Symbol (BPS), when 4QAM and 16QAM CM-VLC schemes are employed, respectively.

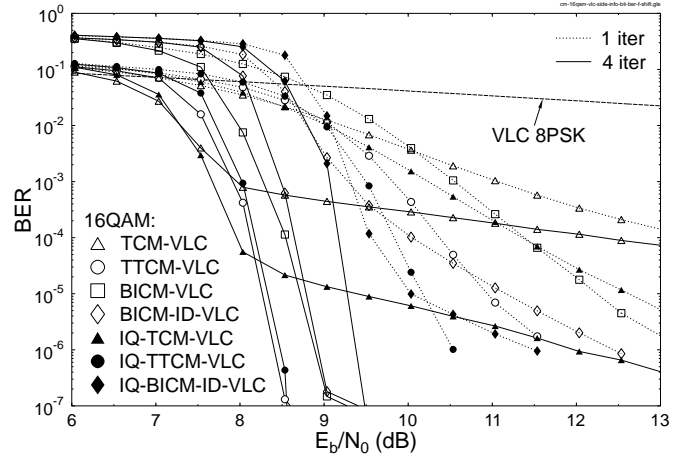


Figure 6: BER versus E_b/N_0 performance of the proposed 16QAM-based (IQ-)CM-VLC schemes and VLC 8PSK, when communicating over **Rayleigh fading channels**. All of these schemes have an effective throughput of **2.61 BPS**.

The Bit Error Ratio (BER) versus signal to noise ratio per bit, namely E_b/N_0 , performance of the proposed schemes having an effective throughput of 2.61 BPS and communicating over AWGN channels is shown in Figure 5. As illustrated in Figure 5, all the CM-VLC schemes attain an iteration gain, when the number of outer iterations is increased from one to four. During the first iteration, before any feedback is provided by the VLC decoder, the best performer at $BER=10^{-5}$ is BICM-ID-VLC, followed by TTCM-VLC, TCM-VLC and BICM-VLC. Owing to the different code structure of the various CM schemes, the iteration gain of each CM-VLC scheme is different. Therefore, after the fourth iteration, the best to poorest performance order has changed to TCM-VLC, TTCM-VLC, BICM-VLC and BICM-ID-VLC. The same performance trends can also be observed in the context of the Symbol Error Ratio (SER) measured in terms of the Levenshtein distance [18], which is defined as the minimum number of insertions, deletions or substitutions required for transforming one symbol sequence into another. However, the SER performance curves were not shown here for reasons of space economy.

The BER versus E_b/N_0 performance of the proposed (IQ-)CM-VLC schemes having an effective throughput of 2.61 BPS and communicating over uncorrelated Rayleigh fading channels is shown in Figure 6. At $BER=10^{-5}$ the best performer during the first iteration is IQ-BICM-ID-VLC, followed by IQ-TTCM-VLC, TTCM-VLC, BICM-ID-VLC, BICM-VLC, IQ-TCM-VLC and TCM-VLC. Again, all schemes benefit from invoking the outer iterative decoding loop. After the fourth iteration, the performance order is TTCM-VLC, IQ-TTCM-VLC, BICM-VLC, BICM-ID-VLC, IQ-BICM-ID-VLC, IQ-TCM-VLC and TCM-VLC.

Note in Figure 6 that during the first iteration, all IQ-CM-VLC schemes exhibit a better performance than their CM-VLC counterparts, which is an added benefit of their IQ-diversity gains. However, the IQ-diversity gain advantage of IQ-TTCM-VLC and IQ-BICM-ID-VLC gradually eroded, as the number of outer iterations was increased from one to four, since a near-Gaussian performance was attained. Nonetheless, as seen in Figure 6, the BER floor of IQ-TTCM-VLC and IQ-BICM-ID-VLC is still lower than that of their non-IQ-interleaved counterparts, exhibiting a BER below 10^{-7} . As shown in Figure 6, the TCM-based 16QAM scheme exhibits an error floor

Code, Modem/BPS	AWGN Channels		Rayleigh Fading Channels	
	E_b/N_0	Gain	E_b/N_0	Gain
VLC, BPSK/0.87	10.12	0.00	44.10	0.00
TCM-VLC, 4QAM/0.87	1.80	8.32	4.02	40.08
TTCM-VLC, 4QAM/0.87	1.68	8.44	3.81	40.29
BICM-VLC, 4QAM/0.87	1.85	8.27	3.67	40.43
BICM-ID-VLC, 4QAM/0.87	1.53	8.59	3.93	40.17
IQ-TCM-VLC, 4QAM/0.87	-	-	3.60	40.50
IQ-TTCM-VLC, 4QAM/0.87	-	-	3.76	40.34
IQ-BICM-ID-VLC, 4QAM/0.87	-	-	3.47	40.63
Perfect coding, 4QAM/0.87	capacity=-0.10		capacity=1.26	
VLC, 8PSK/2.61	13.55	0.00	47.00	0.00
TCM-VLC, 16QAM/2.61	4.99	8.56	17.43	29.57
TTCM-VLC, 16QAM/2.61	5.28	8.27	8.26	38.74
BICM-VLC, 16QAM/2.61	5.39	8.16	8.71	38.29
BICM-ID-VLC, 16QAM/2.61	6.04	7.51	8.78	38.22
IQ-TCM-VLC, 16QAM/2.61	-	-	9.36	37.64
IQ-TTCM-VLC, 16QAM/2.61	-	-	8.32	38.68
IQ-BICM-ID-VLC, 16QAM/2.61	-	-	9.27	37.73
Perfect coding, 16QAM/2.61	capacity=3.53		capacity=5.93	

Table 1: Coding gain values of the proposed (IQ-)CM-VLC schemes. The performance of the best scheme is printed in bold. The term 'perfect coding' refers to unlimited coding and decoding effort [1] which leads to the error-free performance at channel capacity limits.

owing to the existence of uncoded bits in the 16QAM symbol. Although the iterative decoding procedure exchanging information between TCM and VLC subsequently improves the attainable coding gains, the error floor of TCM-VLC after the first and fourth iterations remains similar. On the other hand, the IQ-TCM-VLC scheme is capable of providing a significantly lower error floor compared to that of TCM-VLC. Again, the SER performance curve of CM-VLC exhibits a similar performance trend to that of Figure 6. Specifically, the TTCM-VLC 16QAM scheme utilising four outer iterations is the best performer in terms of both the achievable BER and SER, when communicating over uncorrelated Rayleigh fading channels.

The coding gain values of the proposed schemes using 4QAM and 16QAM after the fourth outer iteration are tabulated in Table 3. When compared to the channel capacity limit of the 4QAM and 16QAM modulation schemes at the effective throughput of 0.87 and 2.61 BPS¹, we can see that most of the proposed schemes have a BER performance about 2 dBs from the corresponding capacity limit. In fact, the proposed BICM-ID-VLC 4QAM scheme is only 1.63 dBs away from the AWGN channel capacity limit of 4QAM at BER= 10^{-5} when attaining an effective throughput of 0.87 BPS.

4. CONCLUSIONS

In this contribution the novel concept of amalgamated source-coding, channel-coding and modulation was proposed. The achievable performance benefits were demonstrated in the context of the novel (IQ-)CM-VLC schemes advocated, which are suitable for transmissions over both AWGN and uncorrelated Rayleigh fading channels. It was shown that the proposed schemes are capable of providing a low BER performance, while performing about 2 dBs from the channel capacity limits at the same effective throughput. Although the additional coding gain provided by the IQ-diversity reduces, as the number of outer iterations increases, nonetheless, a lower error floor is achievable by the IQ-CM-VLC scheme compared to the CM-VLC scheme. It is therefore beneficial to integrate the source-coding, channel-coding

and modulation in an iterative decoding scheme in order to jointly optimise the achievable system performance. Our future work invokes similar schemes in the context of interactive audio and video codecs.

5. REFERENCES

- [1] G. Ungerböck, "Channel coding with multilevel/phase signals," *IEEE Transactions on Information Theory*, vol. 28, pp. 55–67, January 1982.
- [2] L. Hanzo, T. H. Liew and B. L. Yeap, *Turbo Coding, Turbo Equalisation and Space Time Coding for Transmission over Wireless channels*. New York, USA: John Wiley IEEE Press, 2002.
- [3] P. Robertson, T. Würz, "Bandwidth-efficient turbo trellis-coded modulation using punctured component codes," *IEEE Journal on Selected Areas in Communications*, vol. 16, pp. 206–218, February 1998.
- [4] E. Zehavi, "8-PSK trellis codes for a Rayleigh fading channel," *IEEE Transactions on Communications*, vol. 40, pp. 873–883, May 1992.
- [5] G. Caire, G. Taricco and E. Biglieri, "Bit-Interleaved Coded Modulation," *IEEE Transactions on Information Theory*, vol. IT-44, pp. 927–946, May 1998.
- [6] X. Li, J. A. Ritcey, "Bit-interleaved coded modulation with iterative decoding using soft feedback," *IEE Electronics Letters*, vol. 34, pp. 942–943, May 1998.
- [7] S. Al-Semari and T. Fuja, "I-Q TCM: Reliable communication over the Rayleigh fading channel close to the cutoff rate," *IEEE Transactions on Information Theory*, vol. 43, pp. 250–262, January 1997.
- [8] B. D. Jelicic and S. Roy, "Design of trellis coded QAM for flat fading and AWGN channels," *IEEE Transactions on Vehicular Technology*, vol. 44, pp. 192–201, February 1994.
- [9] K. Boulle and J. C. Belfiore, "Modulation scheme designed for the Rayleigh fading channel," in *Proceedings of CISS*, (Princeton, NJ), pp. 288–293, March 1992.
- [10] J. Boutros and E. Viterbo, "Signal Space Diversity: A Power- and Bandwidth-Efficient Diversity Technique for Rayleigh Fading Channel," *IEEE Transactions on Information Theory*, vol. 44, pp. 1453–1467, July 1998.
- [11] S. M. Alamouti, "A simple transmitter diversity scheme for wireless communications," *IEEE Journal on Selected Areas in Communications*, vol. 16, pp. 1451–1458, October 1998.
- [12] S. X. Ng and L. Hanzo, "Space-Time IQ-interleaved TCM and TTCM for AWGN and Rayleigh Fading Channels," *IEE Electronics Letters*, vol. 38, pp. 1553–1555, November 2002.
- [13] S. X. Ng and L. Hanzo, "Space-Time Block Coded IQ-interleaved Joint Coding and Modulation for AWGN and Rayleigh Fading Channels," in *IEEE Vehicular Technology Conference*, (Jeju, Korea), 22–25 April 2003.
- [14] R. Bauer, J. Hagenauer, "On variable length codes for iterative source/channel decoding," in *IEEE Data Compression Conference*, (UT, USA), pp. 273–282, 27–29 March 2001.
- [15] V. B. Balakirsky, "Joint source-channel coding with variable length codes," in *IEEE International Symposium on Information Theory*, (Ulm, Germany), p. 419, 29 June – 4 July 1997.
- [16] Y. Takishima, M. Wada and H. Murakami, "Reversible variable length codes," *IEEE Transactions on Communications*, vol. COM-43, no. 2/3/4, pp. 158–162, 1995.
- [17] A. Chindapol and J. A. Ritcey, "Design, Analysis and Performance Evaluation for BICM-ID with Square QAM Constellations in Rayleigh Fading Channels," *IEEE Journal on Selected Areas in Communications*, vol. 19, pp. 944–957, May 2001.
- [18] T. Okuda, E. Tanaka and T. Kasai, "A method for the correction of garbled words based on the Levenshtein metric," *IEEE Transactions on Computers*, vol. C-25, pp. 172–176, February 1976.

¹These values were computed based on [1, 5].